

# The impacts of different PBL schemes on the simulation of PM<sub>2.5</sub> during severe haze episodes in and surrounding the Jing-Jin-Ji region, China

Tian Li <sup>1</sup>, Hong Wang <sup>2</sup>, Tianliang Zhao <sup>1</sup>, Min Xue <sup>2</sup>, Yaqiang Wang <sup>2</sup>, Huizheng Che <sup>2</sup>, Chao Jiang <sup>3</sup>

1 Collaborative Innovation Center on Forecast and Evaluation of Meteorological Disasters, Key Laboratory for Aerosol-Cloud-Precipitation of China Meteorological Administration, Nanjing University of Information Science and Technology, Nanjing 210044, China

2 State Key Laboratory of Severe Weather/Institute of Atmospheric Composition, Chinese Academy of Meteorological Sciences (CAMS), CMA, Beijing 100081, China

3 Yantai Meteorological Bureau, Yantai 264003, China

Correspondence to: Li Tian (njlitian@126.com) and Wang Hong (wangh@cams.cma.gov.cn)

## Abstract

To explore the impacts of different PBL schemes on the simulation of high PM<sub>2.5</sub> concentrations during severe haze in China, four schemes [Yonsei University (YSU), Mellor-Yamada-Janjic (MYJ), Asymmetric Convection Model, version 2 (ACM2), and Bougeault-Lacarrère (Boulac)] were employed in the Weather Research and Forecasting/Chemistry (WRF-Chem) model to simulate the severe haze that occurred in February 2014 in and surrounding the Jing-Jin-Ji region—one of China's most polluted regions in recent years. The PM<sub>2.5</sub> concentration simulated using the four schemes, together with the meteorological factors closely related to PM<sub>2.5</sub> (wind speed, local vertical diffusion and PBL height), were evaluated through comparison with observations. The simulated results of stations in different terrains were also compared with observations. The results indicated that the eastern plain cities produced better simulation results than the western cities, and the cities under the eastern root of Taihang Mountain produced the worst results in simulating high PM<sub>2.5</sub> concentration in haze. All four schemes simulated very similar daily variation of the surface PM<sub>2.5</sub> concentration compared with observations from 1 to 28 February, 2014. The Boulac scheme was found to be the best among the schemes in terms of its representation of the polluted period, followed by the YSU and MYJ scheme. Owing to its absence of diffusivity in the chemistry module, the surface PM<sub>2.5</sub> concentration simulated using the ACM2 scheme was obviously higher than observed, as well as compared with the three other PBL schemes. The diurnal variations of surface PM<sub>2.5</sub> simulated using the four schemes were not as reasonable as their reflection of daily averaged variation. The simulated concentrations of surface PM<sub>2.5</sub> using the YSU, MYJ and Boulac schemes all showed large negative errors during daytime on polluted days due to their inefficient descriptions of strong local atmospheric stability or extremely weak diffusivity processes under severe haze pollution in Jing-Jin-Ji region. The lower ability of PBL schemes in distinguishing the local PBL meteorologies including daytime diffusion and wind speed between haze and clean days in the complex topography area in China is a main problem for PM<sub>2.5</sub> forecasting, which is worthy of being studied in detail. This also should be noted when the WRF-Chem model is used to simulate and study severe haze pollution in China.

**Keywords:** PM<sub>2.5</sub> simulation, PBL scheme, haze episode, vertical diffusivity, PBL height

## 1. Introduction

Owing to its population explosion, accelerated urbanization, and globalization, China—the country with the fastest growing economy in the world—has been suffering from increasingly severe air pollution since the 1980s. Related to this, haze occurrence in China, on the whole, has continued to grow during the past several decades, especially after 1980 [1]. Today, haze is a frequent phenomenon in most areas of eastern China, leading to adverse economic as well as human health impacts [2]. Broadly, four severe haze regions in China are recognized: Beijing, Tianjin, Hebei Province (abbreviated to Jing-Jin-Ji) and its surroundings [3-5]; the Yangtze River Delta; Pearl River Delta; and the Sichuan Basin. As one of the most important urban agglomerations in China, the Jing-Jin-Ji region and its surroundings has attracted considerable

48 attention recently, because of the serious pollution episodes it has experienced since 2013. Multi-source observations that  
49 can characterize the haze process in Jin-Jin-Ji and its surrounding areas have been used to study the temporal and spatial  
50 variation of haze, meteorological conditions, and the chemical components of haze [6-12]. Based on these extensive  
51 observational studies, continuous studies of the resultant pollution emissions inventory have also been conducted [13-15]. In  
52 addition, a number of simulation studies using atmospheric models have been carried out to study haze and pollutions  
53 processes in China; these studies involve the interactions between meteorological conditions, particle concentrations, and  
54 the variation in the transport characteristics of pollutants during the pollution process [16-20]. There are two key factors  
55 involved in the formation and persistence of haze: one is fine particulate matter ( $PM_{2.5}$ ) and gas pollutants ( $O_3$ ,  $SO_2$ ,  $NO_x$ ,  
56 etc.), and the other is meteorological conditions. Moreover, when modeling haze, there are uncertainties related to the  
57 planetary boundary layer (PBL), which mainly derive from the particular PBL scheme used; and therein, the PBL height  
58 (PBLH), turbulent mixing process, and wind fields are major variables controlling the haze process in the PBL [21-23].  
59 Therefore, the PBL scheme is a vital factor of influence in terms of modeling the formation and maintenance of haze and air  
60 pollution [24, 25]. A lower PBLH and weaker PBL turbulence diffusion are regarded as key meteorological aspects for haze  
61 formation [26]. Studies on different PBL parameterization schemes have shown that an accurate depiction of the  
62 meteorological conditions within the PBL via an appropriate PBL parameterization scheme is important for air pollution  
63 modeling [27-29]. Some studies have also discussed the importance of the PBL scheme in the modeling of  $O_3$   
64 concentrations; specifically, in the U.S.A and using Weather Research and Forecasting/Chemistry model (WRF-Chem)  
65 [30-32]. These studies also touched upon the possible effects of the PBL scheme on the modeling of  $PM_{2.5}$ ; however, little is  
66 known about whether current PBL schemes are efficient in modeling extremely high  $PM_{2.5}$  concentrations and haze events  
67 over the Chinese mainland.

68 In order to investigate the abilities of PBL schemes in modeling  $PM_{2.5}$  over the Jing-Jin-Ji region during serious haze  
69 events with high  $PM_{2.5}$  values, and to provide instructive guidance regarding  $PM_{2.5}$  prediction over this region, separate  
70 WRF-Chem model simulations using four popular PBL schemes [Yonsei University (YSU), Mellor-Yamada-Janjic (MYJ),  
71 Asymmetric Convection Model, version 2 (ACM2), and Bougeault-Lacarrère (Boulac)] were run for haze episodes that  
72 occurred in February 2014. After first introducing the methodology, model configuration and data used, we then evaluate the  
73  $PM_{2.5}$  simulation results from the four PBL schemes by comparing with observations, as well as analyze the related  
74 meteorological fields. Finally, conclusions are drawn regarding the impacts of the PBL on  $PM_{2.5}$  simulation, along with a  
75 discussion on the possible underlying physical mechanisms involved.

## 77 2. Methodology

### 79 2.1 Model Introduction and Configuration

81 The WRF-Chem model is a fully coupled “online” model, with its air quality component fully consistent with the  
82 meteorological component [33, 34]. Version 3.5 of WRF-Chem was employed in this study. Two nested domains (Fig. 1)  
83 were used in the simulation with grid spacing of 27 km and 9 km, respectively. The inner domain was centered at (115 °E,  
84 35.5 °N) on a Lambert map projection. Considering the regional transmission of  $PM_{2.5}$  during haze processes, the main  
85 research area of domain 2 ranged over (111 °E–120.5 °E, 34.5 °N–42.5 °N), containing the whole Jing-Jin-Ji area and its  
86 upstream region including most areas of Shanxi and Shandong provinces and part of Henan Province—both regarded as  
87 contributors to Jing-Jin-Ji’s pollution. The research area is abbreviated as 3JNS hereafter. The two domains used the same  
88 35 vertical levels extending from the surface to 10 hPa, and the layer heights within PBL are showed in Table 3. The  
89 simulation period ranged from 00:00 UTC January 28, 2014 to 00:00 UTC March 1, 2014. The simulation outputs from  
90 February 1 to 28 were used to obtain the chemical component balance from pollutant emissions.

91 The CBM-Z chemistry mechanism [35] combined with MADE/SORGAM (Modal Aerosol Dynamics Model for Europe  
92 and Secondary Organic Aerosol Model) was applied in each domain, and the Fast-J photolysis scheme [36] coupled with  
93 hydrometeors, aerosols and convective parameterizations was chosen. All domains used the RRTM scheme [37] for  
94 longwave radiation, the Goddard scheme for shortwave radiation, the Lin (Purdue) microphysics scheme [38], and the New  
95 Grell scheme for cumulus parameterization (Table 1). Four PBL schemes—YSU, MYJ, ACM2, and Boulac—were adopted  
96 in the model runs.

## 98 2.2 Emissions Intruction

100 The anthropogenic emissions of chemical species, with resolution of  $0.1^\circ \times 0.1^\circ$ , came from the Multi-resolution  
101 Emissions Inventory for China (MEIC) for 2010 (<http://www.meicmodel.org>), which was developed in 2006 for the  
102 INTEX-B mission[13]. The inventory includes 10 major kinds of pollutants and greenhouse gases and more than 700 kinds  
103 of anthropogenic emissions, which can be divided into five sources: transportation, residential, industry, power, and  
104 agricultural. According to the INTEX-B inventory, the main pollutants in China that year were  $\text{SO}_2$ ,  $\text{NO}_x$ , CO, NMVOC,  
105  $\text{PM}_{10}$ ,  $\text{PM}_{2.5}$ , BC, and OC. This 2010 emissions inventory has been validated as credible and widely used in studies of  
106 pollution in China [14, 15, 39].

## 108 2.3 Data Descriptions

110 The National Centers for Environmental Prediction (NCEP) reanalysis data (resolution:  $1^\circ \times 1^\circ$ ) were used for the model's  
111 initial and boundary conditions. The hourly surface  $\text{PM}_{2.5}$  observational data for February 2014 from the China National  
112 Environmental Monitoring Center were used to evaluate the model results. There are 109  $\text{PM}_{2.5}$  sites in domain 2 and 48  
113 sites in 3JNS. The results presented in this paper focus mainly on the sites (evenly distributed) in 3JNS. Surface and vertical  
114 sounding balloon observations of the Meteorological Information Comprehensive Analysis and Process System (MICAPS)  
115 from the China Meteorological Administration were also used for evaluating and analyzing the model. The locations of all  
116 these observational sites in domain 2 are marked in Figure 1. There are 88 MICAPS stations in 3JNS.

117 In order to explore the PBL schemes performance in different area, five stations—Beijing (under the Yan Mountain),  
118 Taiyuan (on the west side of Taihang Mountain), Zhangjiakou (in the northwest of 3JNS), Cangzhou (the coastal station),  
119 and Xingtai (the east foot of Taihang Mountain) were picked up to represent five topography and surface type in the 3JNS.  
120 The location of their abbreviations are displayed in the Figure 1.

## 122 2.4 PBL schemes Introduction

124 PBL schemes can be classified as local or nonlocal closure schemes [40], with the former obtaining the turbulent fluxes  
125 of each grid from mean variables, and the latter by considering the grid and its surroundings. Additionally, nonlocal  
126 schemes are able to simulate the fluxes and profiles of the convective boundary layer. The YSU PBL scheme—an improved  
127 version of the Medium-Range Forecast (MRF) scheme, with a critical bulk Richardson number of 0.25 over land—is a  
128 revised vertical diffusion package with a nonlocal coefficient in the PBL. Compared with the MRF scheme, it increases  
129 boundary layer mixing in the thermally induced free convection regime and decreases it in the mechanically induced forced  
130 convection regime. In addition, this scheme is also a relatively mature scheme that is able to simulate a realistic structure of  
131 the PBL in the WRF model [41, 42]. The MYJ PBL scheme is a turbulent kinetic energy (TKE) local closure scheme that  
132 defines the eddy diffusion coefficients by forecasting the TKE. This scheme is suitable for all stable and weakly unstable  
133 boundary layers [43]. The ACM2 PBL scheme features nonlocal upward mixing and local downward mixing. Compared  
134 with ACM1, it incorporates local turbulent transport and is able to simulate realistic vertical parameter profiles of the PBL  
135 [44]. However, the turbulent diffusion coefficient of ACM2 is not diagnosed in the chemical module (default value of  $1\text{E-}06$ )  
136 [32]; thus, ACM2 is used as a reference scheme for comparing with the other three schemes in detail later in the paper. The  
137 Boulac scheme, regarded as a local closure scheme, has long been regarded as satisfactory in terms of its performance in  
138 orography-induced events[45]. These four PBL schemes are widely used in meso-scale or weather-scale modeling, and their  
139 respective merits and/or shortcomings have been reported in previous studies. They were also selected for use in the present  
140 reported study.

## 142 3. Results and discussion

### 144 3.1 Evaluation of surface $\text{PM}_{2.5}$

146 To validate the efficiencies of the four PBL schemes in simulating  $PM_{2.5}$  in the Jing-Jin-Ji region, the spatial distribution  
147 of the modeled  $PM_{2.5}$  values are compared with observations for a severe and long-lasting haze episode in this region.  
148 Figure 2 displays the averaged  $PM_{2.5}$  distribution from 00:00 UTC February 21 to 00:00 UTC February 25, together with  
149 the observed values during the same period. The period-averaged  $PM_{2.5}$  values reached 300–500  $\mu g m^{-3}$  at observation sites  
150 over this region (marked with dots in Figure 2), and the instantaneous values were even higher; the  $PM_{2.5}$  concentration in  
151 some cities (e.g., Beijing, Xingtai and Tangshan) even reached above 500  $\mu g m^{-3}$  (Figure 3). Furthermore, as shown in  
152 Figure 2 and Figure 3, cities in southern Heibei Province endured more severe pollution than northern areas (e.g., Chengde,  
153 Zhangjiakou). For this haze period, the model results using the four PBL schemes were all reasonable; the observed and  
154 simulated distributions of  $PM_{2.5}$  showed reasonable consistency. The differences in distributions between the YSU, MYJ  
155 and Boulac schemes were small, but the simulation values using the ACM2 scheme were obviously higher than observed.  
156 To evaluate the accuracies of the four PBL schemes in modeling the the variation in  $PM_{2.5}$ , 10 representative cities in 3JNS  
157 were selected (locations displayed in Figure 2), and their hourly variations in  $PM_{2.5}$  concentration, as modeled using the four  
158 PBL schemes, were compared with observations for the period from 00:00 UTC February 1 to 00:00 UTC March 1 (Figure  
159 3). The results show that all four PBL schemes produced similar representations of the real variation in  $PM_{2.5}$  for the whole  
160 of February. As the concentration of  $PM_{2.5}$  is the primary indicators in haze periods, so it can be seen from the Figure 3  
161 that there were two main haze events in February: one from February 13 to 15, and the other from February 21 to 25. The  
162 start and end points of these two events were each modeled well using the four PBL schemes. However, as the simulated  
163 conditions of the second event (February 21 to 25) were more accurate, this one was chosen as the research period in this  
164 study. In terms of the simulations at individual stations, eastern cities (e.g., Hengshui, Cangzhou and Chengde) produced  
165 better simulation results than western cities (e.g., Zhangjiakou, Baoding) for this event overall, suggesting that the PBL  
166 schemes possess properties that are more suited to simulating the  $PM_{2.5}$  concentration in particular localities/regions. As for  
167 how model behaves for particular localities (plains, mountains, or coastal areas, etc.) by using these 4 PBL schemes, we will  
168 discuss about this later. There was little difference in the variation of  $PM_{2.5}$  when using the YSU, MYJ and Boulac schemes,  
169 while the results of ACM2 were obviously higher than those of the other three schemes—attributable to the fact that the  
170 turbulent diffusion was not calculated in the chemistry module.

171 Four statistical indicators [mean bias (MB), normalized mean bias (NMB), normalized mean error (NME), and root mean  
172 square error (RMSE)] of the haze episode, clean days, and whole month averaged over 3JNS were calculated to evaluate the  
173 abilities of the four PBL schemes in simulating  $PM_{2.5}$  (Table 2). The mean and extreme values of haze and clean periods  
174 using each PBL scheme, except ACM2, are also displayed in Table 2. The results show that the  $PM_{2.5}$  modeled during the  
175 haze episode was better than that for the whole month. NB and NMB values of less than zero indicate the model results  
176 were an underestimation of the actual situation. The YSU, MYJ and Boulac schemes underestimated the  $PM_{2.5}$   
177 concentration during daytime but overestimated it at night, the reason for which will be discussed later in the paper. The  
178 Boulac scheme produced the least bias for haze episode compared with the other three schemes, followed by the YSU  
179 scheme, MYJ scheme, and finally the ACM2 scheme. The MB, NMB, NME and RMSE values further illustrate that the  
180 YSU, MYJ and Boulac schemes differed little in terms of their simulation of the  $PM_{2.5}$  concentration during haze. The  
181 simulated values produced by ACM2, however, were much higher than those of the other three schemes.

### 183 **3.2 Relationship between PBL meteorology and $PM_{2.5}$**

184  
185 The daily averaged values of  $PM_{2.5}$  concentration, surface wind speed, PBLH, and vertical diffusivity at level 8 (Table 3)  
186 in 3JNS for the whole of February are showed in Figure 4. The  $PM_{2.5}$  values were determined by averaging the  $PM_{2.5}$  data  
187 of 48 observation stations (Figure 1), and the wind speed values were the average of data of 88 CMA surface monitoring  
188 stations in the same area. The four PBL schemes all showed similar trends as those observed. As indicated by the results in  
189 Figure 4, the  $PM_{2.5}$  modeled using the YSU, MYJ and Boulac schemes showed very little difference. The ACM2 scheme,  
190 however, simulated higher  $PM_{2.5}$  than observed throughout almost the entire month, while its daily variation was  
191 comparable with the other three schemes. The four schemes all simulated similar daily trends for surface wind speed, which  
192 were in agreement with the observed trend, though they were all higher than observed. All four schemes showed the  $PM_{2.5}$   
193 concentration to possess an accurate inverse relationship with wind speed in terms of the daily averaged variation trend. The  
194 daily variation in  $PM_{2.5}$  concentration also possessed a good inverse relationship with the PBLH (averaged over 48 sites,

195 same for vertical diffusion), but not as obviously as that between  $PM_{2.5}$  and surface wind speed. This suggested that a lower  
196 PBLH is an essential prerequisite for haze episodes; but when the PBLH is lower than a certain value, such as 400 m, its  
197 relationship with  $PM_{2.5}$  is not so close. Considering their different diagnoses, the specific values between different PBL  
198 schemes are not comparable, so the focus here is their relationship with  $PM_{2.5}$ , wind speed and vertical diffusivity. The  
199 anti-correlation between the daily  $PM_{2.5}$  and vertical diffusivity of the YSU, MYJ and Boulac schemes was even weaker  
200 than that between  $PM_{2.5}$  and the PBLH, indicating that the impact of local vertical diffusivity on the time scale of the daily  
201 averaged change trend of  $PM_{2.5}$  is limited. Nevertheless, its impact on the hourly change of  $PM_{2.5}$  during the daytime is  
202 clearer and more important, which will be discussed in the section 3.4.

203 To illustrate the modeling performance by using four PBL schemes in different topographies, Figure 5 displays the  
204 simulated and observed daily averaged  $PM_{2.5}$  concentration and wind speed in the whole February of five stations which  
205 can represent five topographies in the 3JNS (Figure 1). It can be seen from the figure that PBL schemes can depict  
206 appropriate variation trends compared with observation as to  $PM_{2.5}$  concentrations and wind speed, and they showed a  
207 good negative correlation with each other. The difference of  $PM_{2.5}$  concentration in YSU, MYJ, and Boulac schemes are  
208 still little in separate stations, and the results by ACM2 schemes are apparently higher than the other three schemes.  
209 Meanwhile, the modeling results in different terrain contain certain differences. In this haze process, the modeling  $PM_{2.5}$   
210 concentrations in some stations are slightly higher than the observations (Beijing, Taiyuan), while some are lower  
211 (Zhangjiakou, Xingtai), and the eastern coastal city (Cangzhou) performed well in this simulation. It is worth mentioning  
212 that the Xingtai station, representing the eastern foot of Taihang Mountain, has obviously lower simulating  $PM_{2.5}$   
213 concentration than the observation by the four schemes, which can be mainly owing to the extremely higher simulation of  
214 wind speed (Fig. 5). Compared with near stations on the eastern Taihang Mountain, it can be found that Shijiazhuang and  
215 Handan also have the similar phenomena (lower simulated  $PM_{2.5}$  and higher simulated wind speed). It should be noted here  
216 that the higher simulated wind speed is one main but probably not the only reason contributing to the higher simulated  
217  $PM_{2.5}$ . In conclusion, the performance of schemes in the eastern root of Taihang Mountain, the most polluted region by  
218 haze in China, were relatively poor due to its specific terrain and complex PBL meteorology. The modeling results in the  
219 eastern plain stations (Cangzhou, etc.) of the 3JNS were better than the west (Zhangjiakou, Xingtai, etc.) as mentioned in  
220 the section 3.1.

221 Figure 6 displays the hourly variations of aera mean  $PM_{2.5}$ , wind speed at 10 m, the PBLH, and vertical diffusivity at  
222 level 8 (Table 3) of the four PBL schemes during the haze episode (total duration: 120 hours). The YSU scheme simulated  
223 the lowest concentration, followed by the Boulac and MYJ schemes, and the ACM2 scheme simulating the highest  
224 concentration. It can be seen from this figure that the  $PM_{2.5}$  concentrations simulated using the YSU, MYJ and Boulac  
225 schemes all possessed good inverse relationships with wind speed at 10 m, the PBLH, and vertical diffusivity. After sunrise,  
226 with the strengthening of solar radiation, the turbulent diffusivity within the PBL continued to enhance, the PBLH and wind  
227 speed also increased, and all three variables reached their maximum at about 07:00 UTC (local 3 o'clock in the afternoon).  
228 After then, all three variables weakened with solar radiation and remained stable at night (after sunset). For the reasons  
229 outlined above, the concentration of simulated  $PM_{2.5}$  during daytime was lower than at night. Owing to the lack of turbulent  
230 diffusivity, the modeled  $PM_{2.5}$  using the ACM2 scheme was not only substantially higher than that of the other three  
231 schemes, but also produced an opposite change trend during the daytime compared with the other three schemes. In  
232 summary, in the model, the effects of vertical diffusion on the hourly change trend of  $PM_{2.5}$  are much more important  
233 compared with the effects on daily averaged  $PM_{2.5}$ .

### 235 3.3 Vertical profiles of $PM_{2.5}$ and meteorology within the PBL

236  
237 The structure of PBL vertical meteorology is very important to particle diffusion, vertical and horizontal transportation,  
238 and thus the simulation of  $PM_{2.5}$ . Unfortunately, air sounding observations are only carried out by the CMA at 00:00 UTC  
239 (early morning, local time) and 12:00 UTC (nightfall), meaning observational data in terms of the vertical profiles of  
240 meteorological parameters during local daytime—local noon (06:00 UTC) especially—are not available and therefore  
241 cannot be used for model validation in China at present. Accordingly, Figure 7 only compares the modeled  $PM_{2.5}$   
242 concentration, wind speed and vertical diffusion using the four PBL schemes. Each value of the profile was first averaged  
243 over the stations in 3JNS, and then averaged over the duration of the haze process (120 hours). The model levels and their

244 corresponding heights are displayed in Table 3. It can be seen from Figure 7 that the differences among the profiles of the  
245 YSU, MYJ and Boulac schemes were small, ranging from  $160 \mu\text{g m}^{-3}$  to  $165 \mu\text{g m}^{-3}$ . The  $\text{PM}_{2.5}$  using the ACM2 scheme  
246 produced higher accumulation at ground level, and its rate of vertical decrease was the largest. The differences between  
247 ACM2 and the three other PBL schemes were obvious. The  $\text{PM}_{2.5}$  values simulated using the ACM2 scheme were much  
248 higher than those of the three other PBL schemes under levels 10–11 (300–400 m), but much smaller above this height. The  
249 discrepancies in the  $\text{PM}_{2.5}$  concentrations and PBL variables among different PBL schemes were mainly apparent beneath  
250 level 11 (height of approximately 402 m). Just under this height local diffusion was strongest, indicating that local vertical  
251 diffusion occurring mainly from 100 m to 400 m, and heights below 400 m, were important for the  $\text{PM}_{2.5}$  simulation. The  
252 results also showed that the surface  $\text{PM}_{2.5}$  concentration was affected by the wind speed and diffusion collectively  
253 throughout the whole PBL (especially under 400 m), rather the surface only.

### 254 3.4 Diurnal variation of surface $\text{PM}_{2.5}$ , emissions and vertical diffusion

255 It can be seen from the discussion on Figure 6 in section 3.2 that the modeling  $\text{PM}_{2.5}$  using ACM2 produced an opposite  
256 change trend during daytime compared with the three other PBL schemes, which was due to there being no calculation of  
257 local particle diffusion in the ACM2 scheme. The diurnal variation of vertical diffusion and  $\text{PM}_{2.5}$  concentration of haze and  
258 clean days using the four PBL schemes is displayed in Figures 8c–8f, along with the diurnal variation of emissions in  
259 Figures 8a and 8b. These figures show exactly how diffusion affected the  $\text{PM}_{2.5}$  trend during the course of one day, from  
260 00:00 UTC to 23:00 UTC. The values of  $\text{PM}_{2.5}$  and diffusion were both averaged over 48  $\text{PM}_{2.5}$  stations in the 3JNS, and  
261 each hour was also averaged during haze (February 21 to 25) and clean periods (February 3 to 5) separately. Most stations’  
262 daily averaged  $\text{PM}_{2.5}$  of observations were above  $200 \mu\text{g m}^{-3}$  in the “haze” while under the  $50 \mu\text{g m}^{-3}$  in the “clean” days.  
263 The diurnal variation produced by the four PBL schemes was exactly the same as shown in Figure 6. The diurnal change  
264 trend of  $\text{PM}_{2.5}$  was largely a synthesis of the change in emissions and vertical diffusion. When diffusion was absent, as in  
265 the ACM2 scheme, the variation of  $\text{PM}_{2.5}$  was extremely close to that of emissions. As such, the concentration of  $\text{PM}_{2.5}$  was  
266 much higher than observed throughout the entire day, but especially during local daytime from 00:00 to 11:00 UTC, both  
267 for haze days (Figure 8e) and clean days (Figure 8f). This indicates that not calculating local particle diffusion during the  
268 daytime may result in higher surface  $\text{PM}_{2.5}$  throughout the entire day, since it prevents particles from moving upward and  
269 therefore results in efficient horizontal transport. The  $\text{PM}_{2.5}$  simulated using the YSU, MYJ and Boulac schemes was  
270 obviously lower than observed during daytime, and their diurnal variation of  $\text{PM}_{2.5}$  disagreed with, and even contrasted with  
271 the observation especially for haze days. Comparing this result with that of the ACM2 scheme, it can be concluded that the  
272 three PBL schemes overestimated the vertical diffusion process in the 3JNS region, leading to lower simulated surface  
273  $\text{PM}_{2.5}$  and negative errors during daytime, particularly when severe haze occurred, which is in agreement with the data  
274 shown in Table 2.

275 There are two reasons for this strong diffusion and lower  $\text{PM}_{2.5}$  during daytime. The direct radiative feedback of aerosols  
276 may lead to weaker diffusion, a more stable atmosphere, and higher surface  $\text{PM}_{2.5}$  when the  $\text{PM}_{2.5}$  concentration is higher  
277 than a certain threshold [26, 46]. However, this feedback was not calculated in the present study. In addition, it was the  
278 calculation methods with respect to vertical diffusion by three of the PBL schemes that led to stronger particle diffusion and  
279 lower surface  $\text{PM}_{2.5}$  than was actually the case in the real atmosphere. Turbulent diffusion is a major factor affecting the  
280 diurnal variation of  $\text{PM}_{2.5}$ , but not the only reason determining concentrations.

281 It should be noted that the different representations of vertical diffusion in these PBL schemes might have different  
282 impacts on  $\text{PM}_{2.5}$  simulation under different conditions of atmospheric stability in different regions. So here, the same five  
283 stations mentioned above were picked up again to illustrate the modeling result of diurnal variations over different  
284 topography (Figure 9). For the small difference of vertical diffusivity between haze and clean period at the five stations, the  
285 figures of diffusion were ignored here. Though there’s no significant pattern in the diurnal variations of observation, this  
286 figure also indicated that the simulated diurnal variations of  $\text{PM}_{2.5}$  of specific stations weren’t as well as daily averaged  
287 variations in Figure 5. Despite this, the modeled trends of Taiyuan and the eastern city Cangzhou were relatively good. By  
288 the influence of Taihang Mountains, Xingtai simulated lower  $\text{PM}_{2.5}$  in haze days and higher  $\text{PM}_{2.5}$  in clean days compared  
289 with observations. When the model performed well in haze with high  $\text{PM}_{2.5}$  concentrations (Taiyuan and Cangzhou), it  
290 simulated apparently higher  $\text{PM}_{2.5}$  in the clean days with lower  $\text{PM}_{2.5}$  concentrations, and vice versa for Zhangjiakou. It  
291  
292

293 seems to be that the little difference of diffusivity calculation between haze and clean days by all the PBL schemes  
294 calculation might lead to this interesting phenomenon, which is probably the main way to improve PM<sub>2.5</sub> forecasting in  
295 complex topography.

## 296 **4 Conclusion**

297 To explore the impacts of different PBL schemes on PM<sub>2.5</sub> simulation, four PBL schemes (YSU, MYJ, ACM2, Boulac)  
298 were applied in the WRF-Chem model to simulate haze episodes that occurred in the Jing-Jin-Ji region and its surroundings  
299 of China. The research area is abbreviated to 3JNS in this paper.

300 The results of the four PBL schemes in simulating the PM<sub>2.5</sub> concentration over 3JNS showed that all four schemes  
301 performed similarly with respect to the PM<sub>2.5</sub> trend during a month that included haze episodes. However, among them, the  
302 Boulac scheme produced the least bias for haze period, followed by the YSU and MYJ scheme, and these three schemes  
303 showed negligible difference in simulating the PM<sub>2.5</sub> concentration. Owing to the lack of diffusivity in the chemistry  
304 module, the PM<sub>2.5</sub> concentration simulated using the ACM2 scheme was higher than observed, and higher than that  
305 simulated in the three other schemes. All four PBL schemes simulated similar daily trends in PM<sub>2.5</sub> concentration, which  
306 was in agreement with the observation and possessed a good inverse relationship with the PBLH and wind speed—better  
307 than with vertical diffusion. All the PBL schemes behaves diversely in different terrains. On the whole, eastern plain cities  
308 such as Cangzhou and Chengde produced better simulation results than the western cities such as Zhangjiakou and Baoding  
309 which near mountains; the cities under the eastern root of Taihang Mountain produced the worst results in simulating high  
310 PM<sub>2.5</sub> and wind speed; the modeling results of plain cities were better than the cities under the mountain (e.g. Beijing under  
311 the Yan Mountain). Study results showd that all the four PBL schemes hadn't enough ability in distinguishing the local PBL  
312 meteorologies including daytime diffusion and wind speed between haze and clean days in the complex topography area in  
313 China, which may be regarded as an important direction for the improving of PM<sub>2.5</sub> simulation. The heights under or near  
314 the 400 m were found to be very important for PM<sub>2.5</sub> simulation. The PM<sub>2.5</sub> concentration simulated using the ACM2  
315 scheme produced higher accumulation at ground level, and its rate of vertical decrease was the largest among all the  
316 schemes. ACM2 was used as a reference scheme for comparison with the three other schemes, to describe the diurnal  
317 impacts of vertical diffusion on PM<sub>2.5</sub> simulation. The effects of vertical diffusion on the hourly change trend of PM<sub>2.5</sub>  
318 simulation were far more important than those on the simulation of daily averaged PM<sub>2.5</sub>. Diurnal variation of PM<sub>2.5</sub> was  
319 largely a synthesis of the change in emissions and vertical diffusion. If lacking diffusivity, as with the ACM2 scheme, the  
320 diurnal variation of PM<sub>2.5</sub> and emissions were similar and the PM<sub>2.5</sub> concentration for the whole day was overestimated.  
321 Compared with the ACM2 scheme, the three other PBL schemes overestimated the vertical diffusion process in the 3JNS,  
322 leading to a lower simulation of surface PM<sub>2.5</sub> and negative errors during daytime—partically when severe haze occurred. In  
323 addition, the small gap of diffusivity between haze and clean days by PBL schemes may lead to the errors in simulating  
324 PM<sub>2.5</sub> concentrations.

325 Though the differences in PM<sub>2.5</sub> concentration among the PBL scehmes were very small, the exact reasons related to  
326 these differences were not discussed in this study. The reasons for the poor reflection of diurnal variation in the PBL  
327 schemes, resulting in PM<sub>2.5</sub> errors in numerical models, need to be studied in detail, and then adjustments made to improve  
328 results for different regions.

## 329 **Conflict of Interest**

330 The authors declare that there is no conflict of interest regarding the publication of this article.

## 331 **Acknowledgments:**

332 This work is supported by National Natural Scientific Foundation of China (41275007), 973 Program of Ministry of Science  
333 and Technology of China (2014CB441201), National Science and Technology Project of China (2014BAC22B04).

## 334 **References**

- 340 [1] Y. Ding and Y. Liu, "Analysis of long-term variations of fog and haze in China in recent 50 years and their relations with  
341 atmospheric humidity," *Science China Earth Sciences*, vol. 57, no. 1, pp. 36-46, 2013.  
342
- 343 [2] M. Li and L. Zhang, "Haze in China: current and future challenges," *Environmental pollution*, vol. 189, no., pp. 85-6, 2014.  
344
- 345 [3] H. Che, X. Zhang, Y. Li, et al., "Haze trends over the capital cities of 31 provinces in China, 1981–2005," *Theoretical and  
346 Applied Climatology*, vol. 97, no. 3-4, pp. 235-42, 2008.  
347
- 348 [4] P. Zhao, X. Zhang, X. Xu, et al., "Long-term visibility trends and characteristics in the region of Beijing, Tianjin, and Hebei,  
349 China," *Atmospheric Research*, vol. 101, no. 3, pp. 711-8, 2011.  
350
- 351 [5] F. Chai, J. Gao, Z. Chen, et al., "Spatial and temporal variation of particulate matter and gaseous pollutants in 26 cities in  
352 China," *Journal of Environmental Sciences*, vol. 26, no. 1, pp. 75-82, 2014.  
353
- 354 [6] X. Y. Zhang, Y. Q. Wang, T. Niu, et al., "Atmospheric aerosol compositions in China: spatial/temporal variability, chemical  
355 signature, regional haze distribution and comparisons with global aerosols," *Atmospheric Chemistry and Physics*, vol. 12,  
356 no. 2, pp. 779-99, 2012.  
357
- 358 [7] Q. Zhang, Z. Shen, J. Cao, et al., "Variations in PM<sub>2.5</sub>, TSP, BC, and trace gases (NO<sub>2</sub>, SO<sub>2</sub>, and O<sub>3</sub>) between haze and  
359 non-haze episodes in winter over Xi'an, China," *Atmospheric Environment*, vol. 112, no., pp. 64-71, 2015.  
360
- 361 [8] X. Fu, S. X. Wang, Z. Cheng, et al., "Source, transport and impacts of a heavy dust event in the Yangtze River Delta, China, in  
362 2011," *Atmos Chem Phys*, vol. 14, no. 3, pp. 1239-54, 2014.  
363
- 364 [9] X. Wang, J. Chen, J. Sun, et al., "Severe haze episodes and seriously polluted fog water in Ji'nan, China," *The Science of the  
365 total environment*, vol. 493, no., pp. 133-7, 2014.  
366
- 367 [10] P. S. Zhao, F. Dong, D. He, et al., "Characteristics of concentrations and chemical compositions for PM<sub>2.5</sub> in the region of  
368 Beijing, Tianjin, and Hebei, China," *Atmos Chem Phys*, vol. 13, no. 9, pp. 4631-44, 2013.  
369
- 370 [11] M. Tao, L. Chen, Z. Wang, et al., "A study of urban pollution and haze clouds over northern China during the dusty season  
371 based on satellite and surface observations," *Atmospheric Environment*, vol. 82, no. 0, pp. 183-92, 2014.  
372
- 373 [12] H. Wang, S.-C. Tan, Y. Wang, et al., "A multisource observation study of the severe prolonged regional haze episode over  
374 eastern China in January 2013," *Atmospheric Environment*, vol. 89, no. 0, pp. 807-15, 2014.  
375
- 376 [13] Q. Zhang, D. G. Streets, G. R. Carmichael, et al., "Asian missions in 2006 for the NASA INTEX-B mission," *Atmos. Chem.  
377 Phys.*, vol. 9, no., pp. 5131-5153, 2009.  
378
- 379 [14] S. Wang, D. G. Streets, Q. Zhang, et al., "Satellite detection and model verification of NO<sub>x</sub> emissions from power plants in  
380 Northern China," *Environmental Research Letters*, vol. 5, no. 4, pp. 044007, 2010.  
381
- 382 [15] M. Li, Q. Zhang, D. G. Streets, et al., "Mapping Asian anthropogenic emissions of non-methane volatile organic compounds  
383 to multiple chemical mechanisms," *Atmospheric Chemistry and Physics*, vol. 14, no. 11, pp. 5617-38, 2014.  
384
- 385 [16] Z. Wang, J. Li, Z. Wang, et al., "Modeling study of regional severe hazes over mid-eastern China in January 2013 and its  
386 implications on pollution prevention and control," *Science China Earth Sciences*, vol. 57, no. 1, pp. 3-13, 2013.  
387
- 388 [17] Y. Gao, M. Zhang, Z. Liu, et al., "Modeling the feedback between aerosol and meteorological variables in the atmospheric

- 389 boundary layer during a severe fog–haze event over the North China Plain," *Atmospheric Chemistry and Physics*, vol. 15,  
390 no. 8, pp. 4279-95, 2015.
- 391
- 392 [18] X. Tie, Q. Zhang, H. He, et al., "A budget analysis of the formation of haze in Beijing," *Atmospheric Environment*, vol. 100,  
393 no., pp. 25-36, 2015.
- 394
- 395 [19] Q. Zhang, C. Zhao, X. Tie, et al., "Characterizations of aerosols over the Beijing region: A case study of aircraft  
396 measurements," *Atmospheric Environment*, vol. 40, no. 24, pp. 4513-27, 2006.
- 397
- 398 [20] G. J. Zheng, F. K. Duan, H. Su, et al., "Exploring the severe winter haze in Beijing: the impact of synoptic weather, regional  
399 transport and heterogeneous reactions," *Atmospheric Chemistry and Physics*, vol. 15, no. 6, pp. 2969-83, 2015.
- 400
- 401 [21] J. Quan, X. Tie, Q. Zhang, et al., "Characteristics of heavy aerosol pollution during the 2012–2013 winter in Beijing, China,"  
402 *Atmospheric Environment*, vol. 88, no., pp. 83-9, 2014.
- 403
- 404 [22] C. M. Gan, Y. Wu, B. L. Madhavan, et al., "Application of active optical sensors to probe the vertical structure of the urban  
405 boundary layer and assess anomalies in air quality model PM<sub>2.5</sub> forecasts," *Atmospheric Environment*, vol. 45, no. 37, pp.  
406 6613-21, 2011.
- 407
- 408 [23] Q. Zhang, J. Quan, X. Tie, et al., "Effects of meteorology and secondary particle formation on visibility during heavy haze  
409 events in Beijing, China," *The Science of the total environment*, vol. 502, no., pp. 578-84, 2015.
- 410
- 411 [24] H. He, X. Tie, Q. Zhang, et al., "Analysis of the causes of heavy aerosol pollution in Beijing, China: A case study with the  
412 WRF-Chem model," *Particuology*, vol. 20, no. 0, pp. 32-40, 2015.
- 413
- 414 [25] J. Quan, Y. Gao, Q. Zhang, et al., "Evolution of planetary boundary layer under different weather conditions, and its impact  
415 on aerosol concentrations," *Particuology*, vol. 11, no. 1, pp. 34-40, 2013.
- 416
- 417 [26] H. Wang, M. Xue, X. Y. Zhang, et al., "Mesoscale modeling study of the interactions between aerosols and PBL meteorology  
418 during a haze episode in Jing–Jin–Ji (China) and its nearby surrounding region – Part 1: Aerosol distributions and  
419 meteorological features," *Atmospheric Chemistry and Physics*, vol. 15, no. 6, pp. 3257-75, 2015.
- 420
- 421 [27] X. M. Hu, P. M. Klein and M. Xue, "Evaluation of the updated YSU planetary boundary layer scheme within WRF for wind  
422 resource and air quality assessments," *Journal of Geophysical Research: Atmospheres*, vol. 118, no. 18, pp.  
423 10,490-10,505, 2013.
- 424
- 425 [28] X. M. Hu, J. W. Nielsen-Gammon and F. Zhang, "Evaluation of Three Planetary Boundary Layer Schemes in the WRF  
426 Model," *Journal of Applied Meteorology and Climatology*, vol. 49, no. 9, pp. 1831-44, 2010.
- 427
- 428 [29] X. M. Hu, F. Zhang and J. W. Nielsen-Gammon, "Ensemble-based simultaneous state and parameter estimation for treatment  
429 of mesoscale model error: A real-data study," *Geophysical Research Letters*, vol. 37, no. 8, pp. n/a-n/a, 2010.
- 430
- 431 [30] X. M. Hu, P. M. Klein, M. Xue, et al., "Impact of Low-Level Jets on the Nocturnal Urban Heat Island Intensity in Oklahoma  
432 City," *Journal of Applied Meteorology and Climatology*, vol. 52, no. 8, pp. 1779-802, 2013.
- 433
- 434 [31] X. M. Hu, P. M. Klein, M. Xue, et al., "Impact of the vertical mixing induced by low-level jets on boundary layer ozone  
435 concentration," *Atmospheric Environment*, vol. 70, no., pp. 123-30, 2013.
- 436
- 437 [32] X. M. Hu, D. C. Doughty, K. J. Sanchez, et al., "Ozone variability in the atmospheric boundary layer in Maryland and its

438 implications for vertical transport model," *Atmospheric Environment*, vol. 46, no., pp. 354-64, 2012.

- 439
- 440 [33] G. A. Grell, S. E. Peckham, R. Schmitz, et al., "Fully coupled "online" chemistry within the WRF model," *Atmospheric*
- 441 *Environment*, vol. 39, no. 37, pp. 6957-75, 2005.
- 442
- 443 [34] J. D. Fast, W. I. Gustafson, R. C. Easter, et al., "Evolution of ozone, particulates, and aerosol direct radiative forcing in the
- 444 vicinity of Houston using a fully coupled meteorology-chemistry-aerosol model," *Journal of Geophysical Research:*
- 445 *Atmospheres*, vol. 111, no. D21, pp. D21305, 2006.
- 446
- 447 [35] R. A. Zaveri and L. K. Peters, "A new lumped structure photochemical mechanism for large-scale applications," *Journal of*
- 448 *Geophysical Research*, vol. 104, no. D23, pp. 30387, 1999.
- 449
- 450 [36] Oliver Wild, Xin Zhu and Michael J. Prather. "Fast-J: Accurate simulation of in- and below-cloud photolysis in tropospheric
- 451 chemical models," *Journal of Atmospheric Chemistry*, vol. 37, no., pp. 245-282, 2000.
- 452
- 453 [37] E. J. Mlawer, S. J. Taubman, P. D. Brown, et al., "Radiative transfer for inhomogeneous atmospheres: RRTM, a validated
- 454 correlated-k model for the longwave," *Journal of Geophysical Research*, vol. 102, no. D14, pp. 16663, 1997.
- 455
- 456 [38] Y. L. Lin, R. D. Farley and H. D. Orville, "Bulk Parameterization of the Snow Field in a Cloud Model," *Journal of Climate*
- 457 *and Applied Meteorology*, vol. 22, no. 6, pp. 1065-92, 1983.
- 458
- 459 [39] S. W. Wang, Q. Zhang, D. G. Streets, et al., "Growth in NO<sub>x</sub> emissions from power plants in China: bottom-up estimates and
- 460 satellite observations," *Atmospheric Chemistry and Physics*, vol. 12, no. 10, pp. 4429-47, 2012.
- 461
- 462 [40] B. Xie, J. C. H. Fung, A. Chan, et al., "Evaluation of nonlocal and local planetary boundary layer schemes in the WRF
- 463 model," *Journal of Geophysical Research: Atmospheres*, vol. 117, no. D12, pp. D12103, 2012.
- 464
- 465 [41] Songyou Hong and Ying Noh. "A new vertical diffusion package with an explicit treatment of entrainment processes,"
- 466 *Monthly Weather Review*, vol. 134, no., pp. 2318-2341, 2006.
- 467
- 468 [42] Songyou Hong and Hualu Pan. "Nonlocal Boundary Layer Vertical diffusion in a medium-range forecast model," *Monthly*
- 469 *Weather Review*, vol. 124, no., pp. 2322-2339, 1996.
- 470
- 471 [43] Zavisla I. Janjic. "The step-mountain eta coordinate model: further developments of the convection, viscous sublayer, and
- 472 turbulence closure schemes," *Monthly Weather Review*, vol. 122, no., pp. 927-945, 1994.
- 473
- 474 [44] J. E. Pleim, "A Combined Local and Nonlocal Closure Model for the Atmospheric Boundary Layer. Part I: Model Description
- 475 and Testing," *Journal of Applied Meteorology and Climatology*, vol. 46, no. 9, pp. 1383-95, 2007.
- 476
- 477 [45] P. Bougeault and P. Lacarrère, "Parameterization of orography-induced turbulence in a mesobeta-scale model," *Monthly*
- 478 *Weather Review*, vol. 117, no., pp. 1872-1890, 1989.
- 479
- 480 [46] H. Wang, G. Y. Shi, X. Y. Zhang, et al., "Mesoscale modelling study of the interactions between aerosols and PBL
- 481 meteorology during a haze episode in China Jing-Jin-Ji and its near surrounding region – Part 2: Aerosols' radiative
- 482 feedback effects," *Atmospheric Chemistry and Physics*, vol. 15, no. 6, pp. 3277-87, 2015.
- 483
- 484

485  
486

Table 1. Main physical schemes used in WRF-Chem.

Physical process	Physics option
Shortwave radiation	Goddard
Longwave radiation	RRTM
Microphysics	Lin
Cumulus parameterization	New Grell scheme
	YSU
	MYJ
Planetary boundary layer	ACM2
	Boulac
Surface layer	Revised MM5 Monin–Obukhov for YSU, ACM2, and Boulac Monin–Obukhov for MYJ
Land surface	Unified Noah Land-Surface Model

487  
488  
489  
490

Table 2. Comparisons of statistical indicators of PM<sub>2.5</sub>

(Haze: Feb 21 to 25 – daytime, 00:00–11:00 UTC; night, 12:00–24:00 UTC. Clean days: Feb 3 to 5. Unit:  $\mu\text{g m}^{-3}$ )

	YSU		MYJ		ACM2		Boulac	
	MB	NMB	MB	NMB	MB	NMB	MB	NMB
Whole month	17.7	15.9%	24.5	22.0%	54.9	49.2%	21.2	19.0%
Haze episode	-2.5	-1.4%	5.4	3.0%	47.3	26.7%	0.13	0.5%
Haze daytime	-11.8	-6.8%	-1.8	-1.0%	58.6	33.6%	-8.1	-4.6%
Haze night	7.2	4.0%	13.2	7.3%	35.3	19.6%	8.9	4.9%
	NME	RMSE	NME	RMSE	NME	RMSE	NME	RMSE
Whole month	49.8%	104.0	52.5%	106.0	68.7%	119.3	49.8%	103.8
Haze episode	31.2%	76.6	31.4%	75.4	40.9%	92.6	31.2%	74.6
Haze daytime	31.0%	76.6	30.6%	73.9	45.2%	98.7	30.6%	75.8
Haze night	31.4%	76.6	32.1%	76.9	36.4%	85.6	31.8%	77.5
Haze / clean	174.4 / 64.9		182.4 / 70.4				177.1 / 69.2	
	Haze	Clean	Haze	Clean			Haze	Clean
Maximum	217.8	22.2	220.5	30.4			220.6	27.6
Minimum	98.1	24.4	100.2	26.7			105.8	28.5

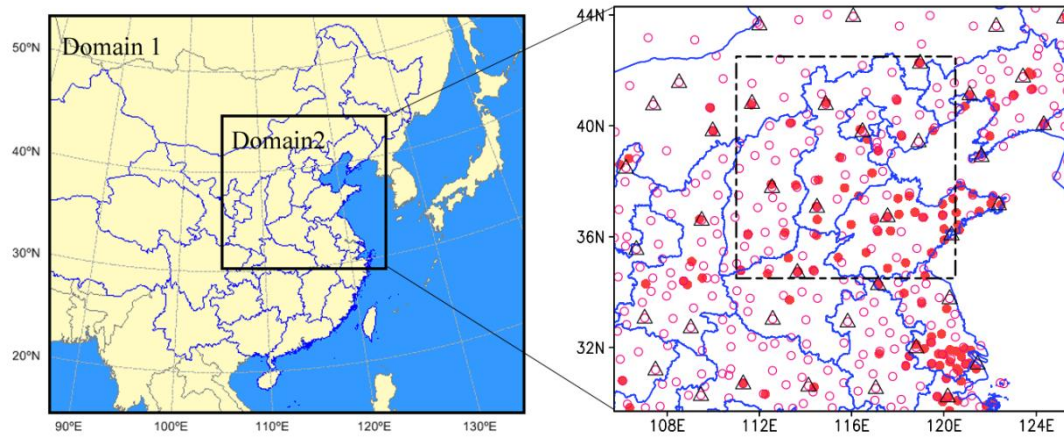
491  
492  
493

Table 3. Model levels and their corresponding heights.

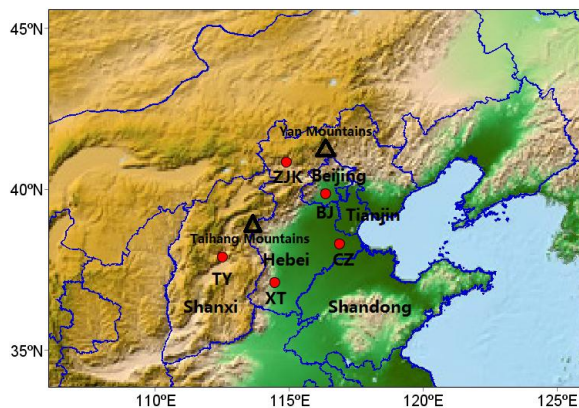
Model Level	1	2	3	4	5	6	7	8	9	10	11	12	13	14	15	16	17
Geopotential height (m)	0	15	30	45	61	91	137	175	222	315	402	586	767	943	1132	1307	1496

494  
495

496 Figure Captions:  
497 Figure 1. Nested modeling domains (left), the distribution of observation sites within domain 2 (right: filled circles,  $PM_{2.5}$   
498 observation sites; open circles, surface meteorological sites; open triangles: upper-air meteorological stations; the  
499 dashed-line square area represents the research area (3JNS) referred to.) and the topography of the research area  
500 (bottom).  
501 Figure 2. Mean simulated (shaded) and observed (dotted)  $PM_{2.5}$  values during the haze period (Feb 21 to 25).  
502 Figure 3. Simulated and observed hourly  $PM_{2.5}$  concentration at 10 sites in February 2014.  
503 Figure 4. Variation of the daily averaged  $PM_{2.5}$  concentration, wind speed (near-surface), PBLH, and vertical diffusivity of  
504 the area mean in February.  
505 Figure 5. Variation of the daily averaged  $PM_{2.5}$  concentration and wind speed (near-surface) at 5 sites of different terrain in  
506 February  
507 Figure 6. Variation of the area-averaged  $PM_{2.5}$  concentration, wind speed at 10m, PBLH, and vertical diffusivity during the  
508 haze process.  
509 Figure 7. Vertical profiles of the  $PM_{2.5}$  concentration, wind speed, and vertical diffusivity.  
510 Figure 8. Diurnal variation of emissions,  $PM_{2.5}$ , and vertical diffusion.  
511 Figure 9. Diurnal variation of  $PM_{2.5}$  in polluted and clean process at 5 sites of different terrain.  
512



513



514

515

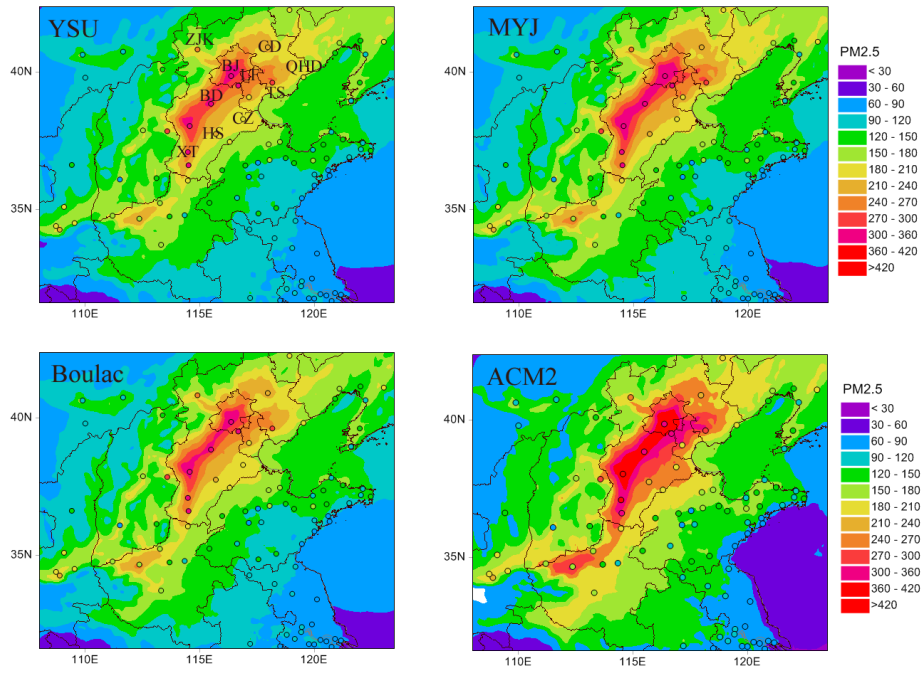
516

517

518

519

Figure 1. Nested modeling domains (left), the distribution of observation sites within domain 2 (right: filled circles,  $PM_{2.5}$  observation sites; open circles, surface meteorological sites; open triangles: upper-air meteorological stations; the dashed-line square area represents the research area (3JNS) referred to.) and the topography of the research area (bottom).



520  
521  
522

Figure 2. Mean simulated (shaded) and observed (dotted) PM<sub>2.5</sub> values during the haze period (Feb 21 to 25).

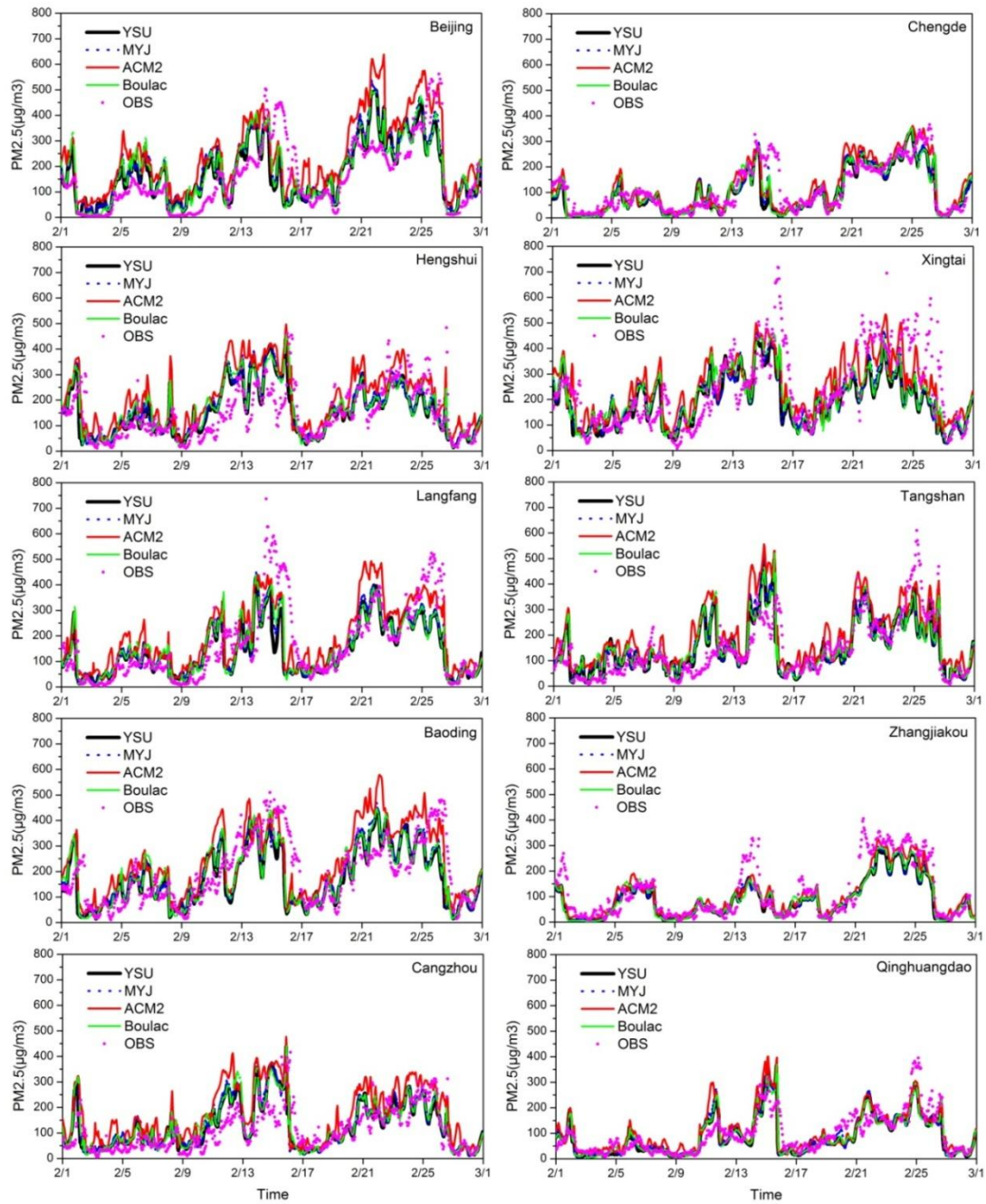
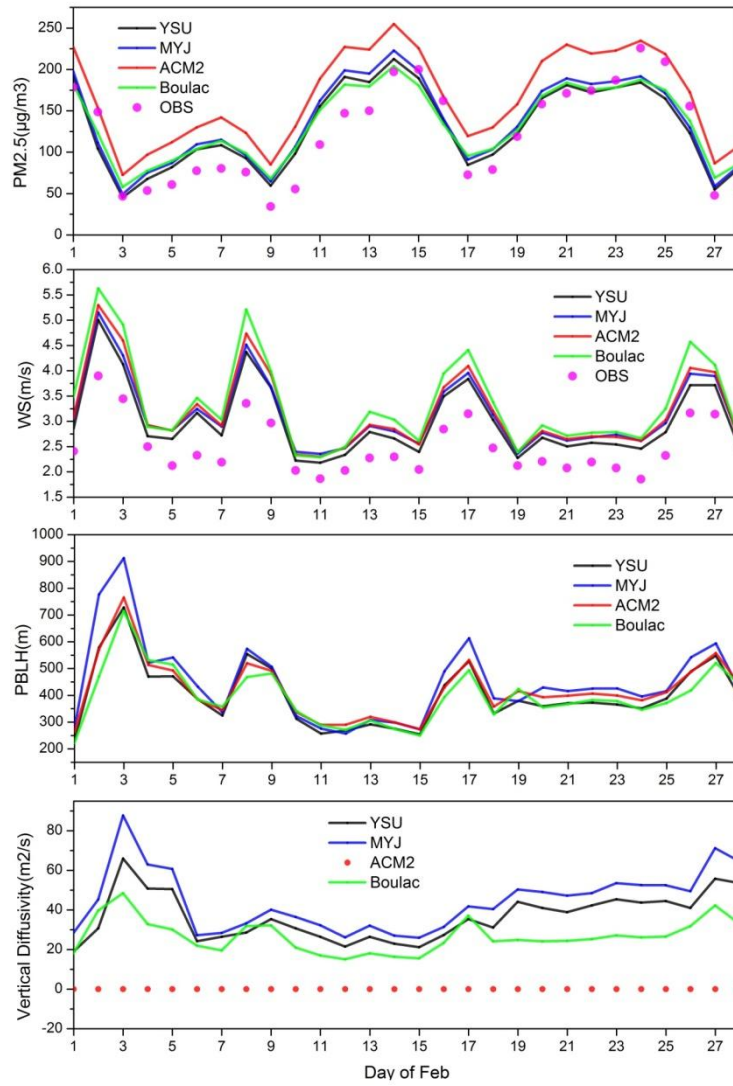


Figure 3. Simulated and observed hourly  $PM_{2.5}$  concentration at 10 sites in February 2014.

523

524

525



526

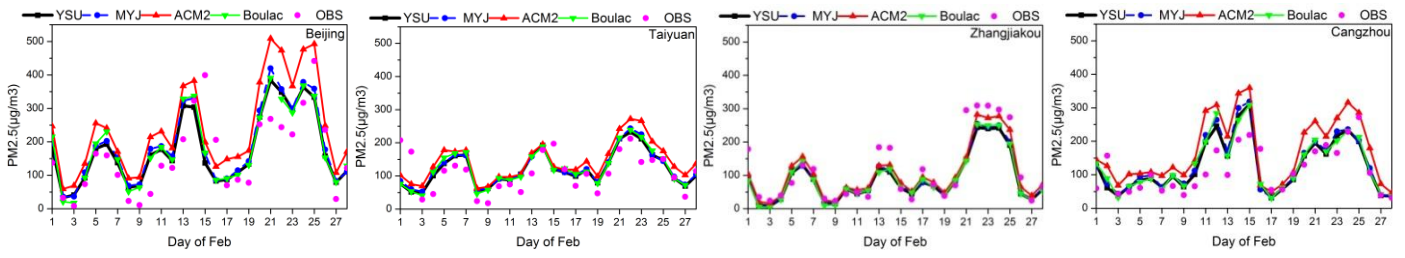
527

528

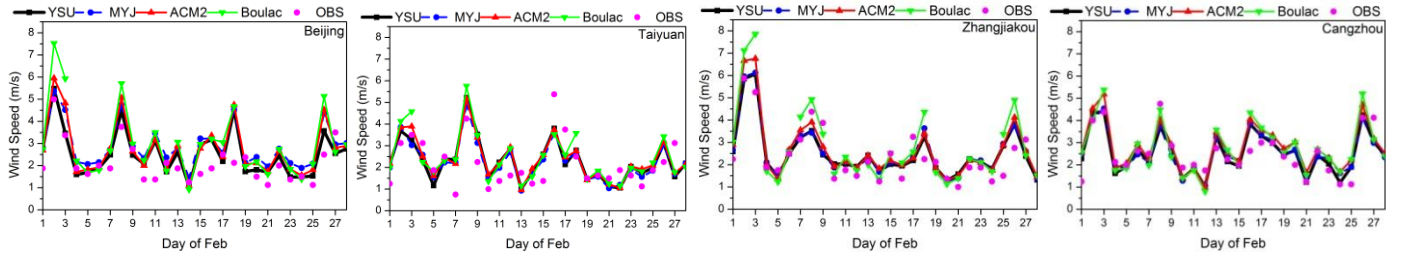
529

Figure 4. Variation of the daily averaged PM<sub>2.5</sub> concentration, wind speed (near-surface), PBLH, and vertical diffusivity of the area mean in February.

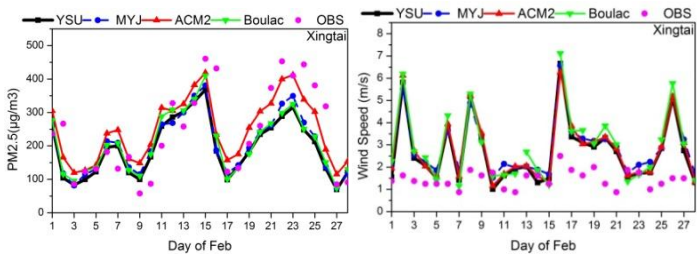
530



531



532



533

534

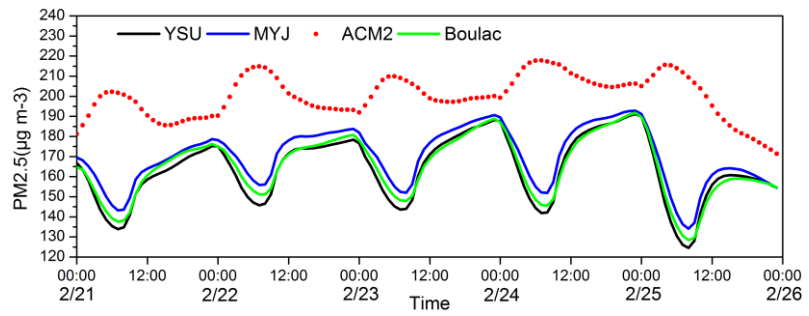
Fig 5. Variation of the daily averaged PM<sub>2.5</sub> concentration and wind speed (near-surface) at 5 sites of different terrain in Febuary

535

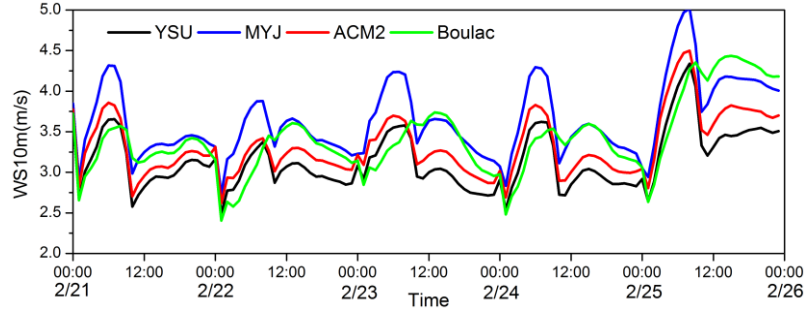
536

537

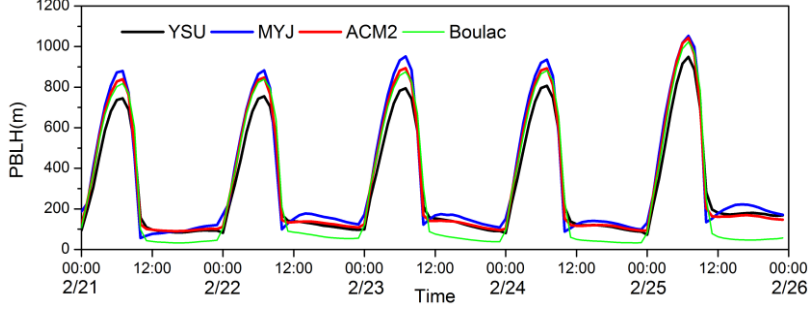
538



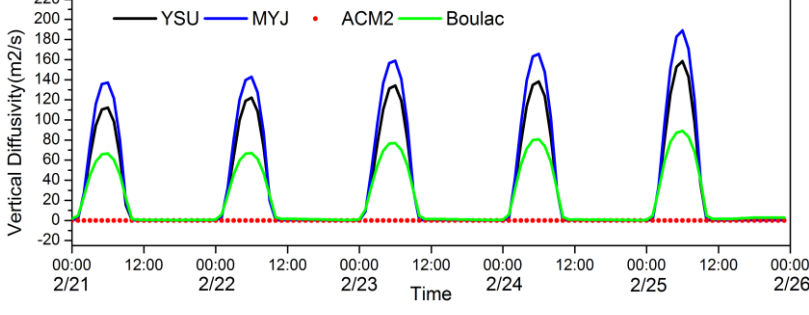
539



540



541



542

543

544

545

Figure 6. Variation of the area-averaged  $PM_{2.5}$  concentration, wind speed at 10m, PBLH, and vertical diffusivity during the haze process.

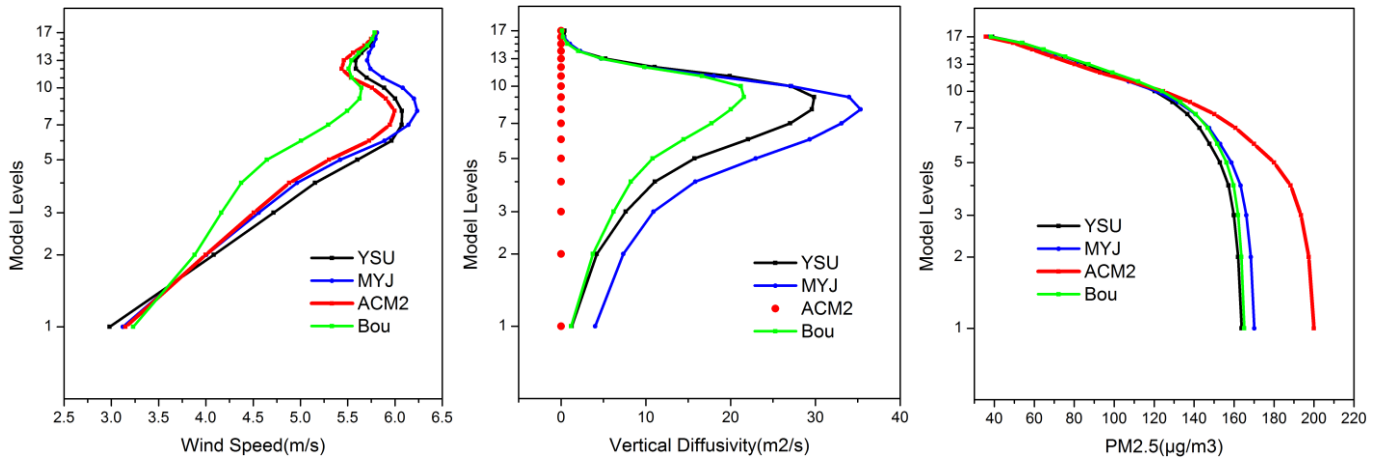
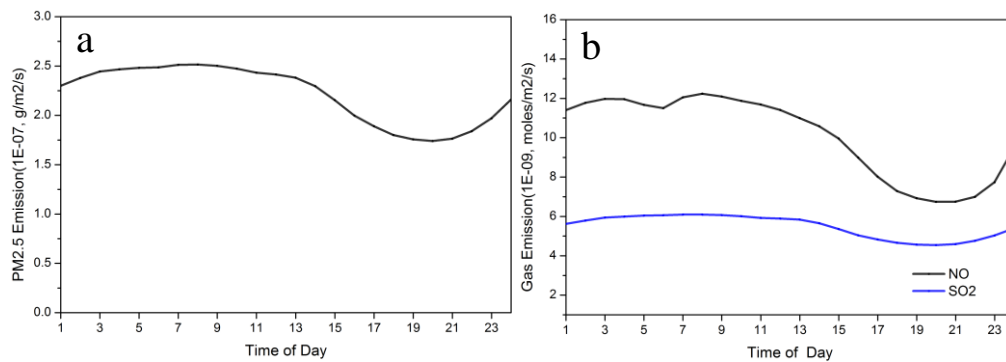


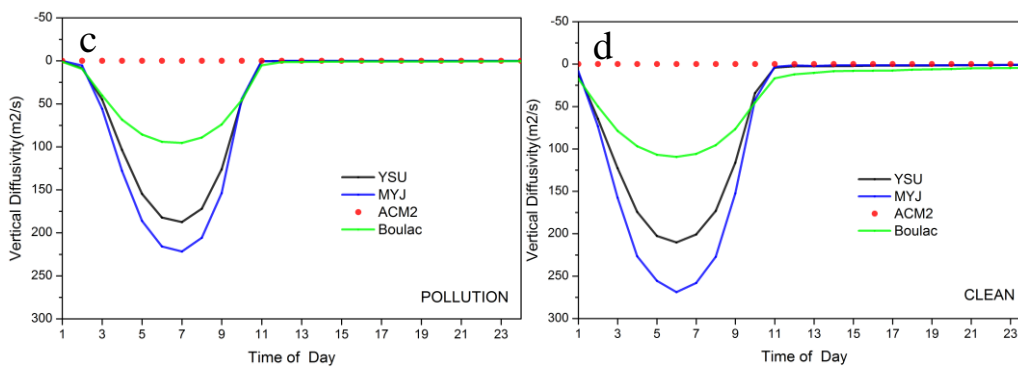
Figure 7. Vertical profiles of the PM<sub>2.5</sub> concentration, wind speed, and vertical diffusivity.

546  
547  
548

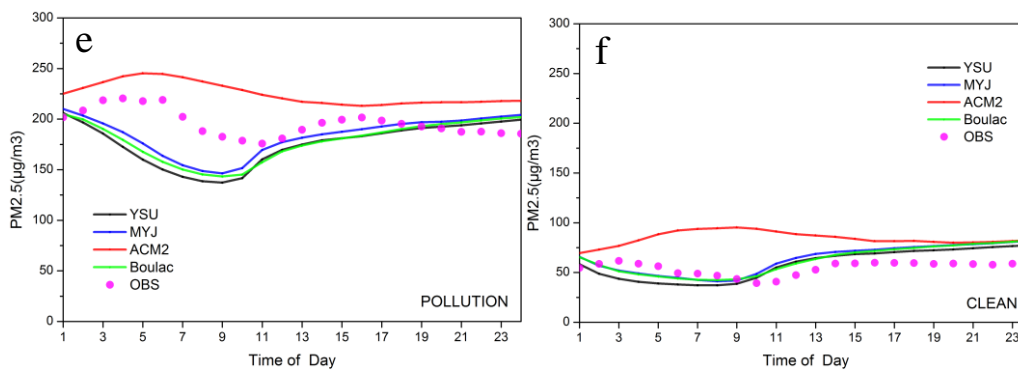
549



550



551



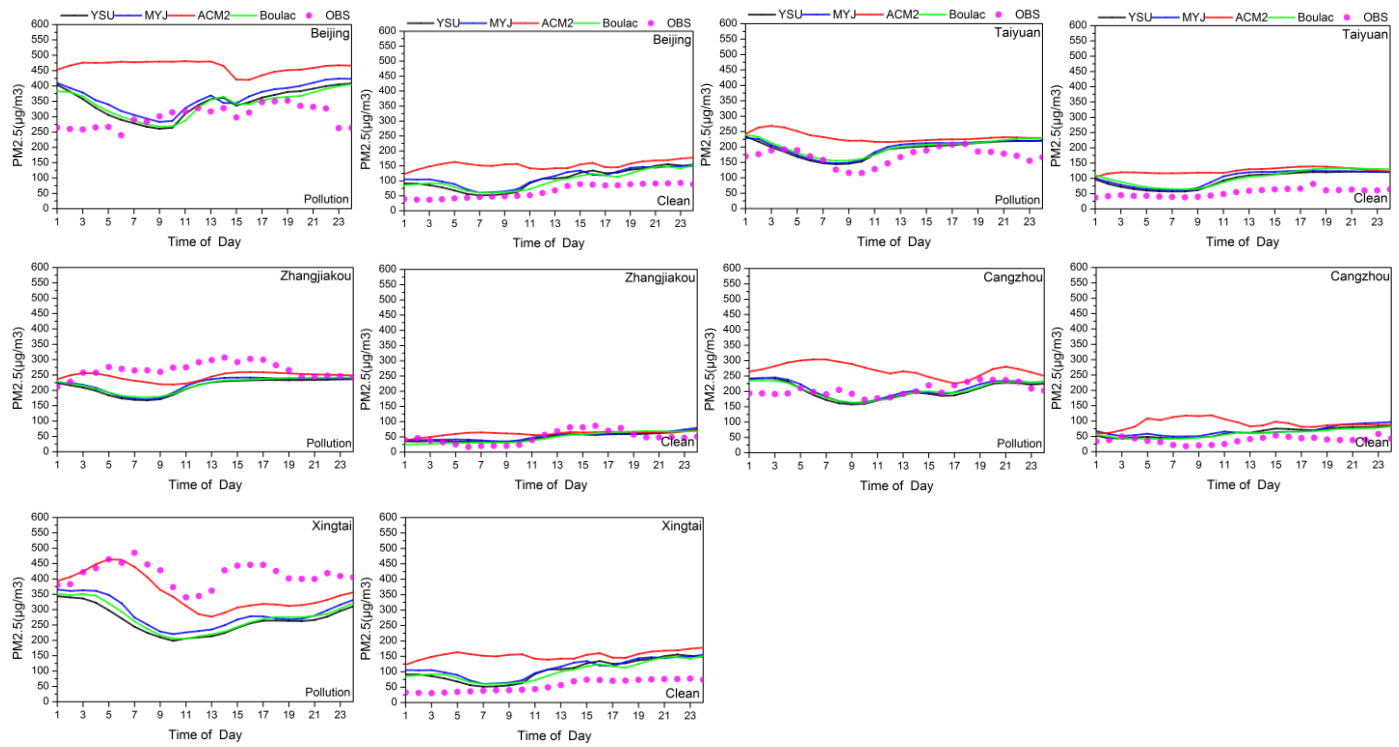
552

553

554

Figure 8. Diurnal variation of emissions, PM<sub>2.5</sub>, and vertical diffusion

555



556

557

558

559

Figure 9. Diurnal variation of PM<sub>2.5</sub> in polluted and clean process at 5 sites of different terrain.